HHS Public Access

Author manuscript

Genesis. Author manuscript; available in PMC 2019 December 26.

Published in final edited form as:

Genesis. 2019 January ; 57(1): e23264. doi:10.1002/dvg.23264.

Cadherin-7 mediates proper neural crest cell-placodal neuron interactions during trigeminal ganglion assembly

Chyong-Yi Wu, **Lisa A. Taneyhill**

Department of Animal and Avian Sciences, University of Maryland, College Park, Maryland

Summary

The cranial trigeminal ganglia play a vital role in the peripheral nervous system through their relay of sensory information from the vertebrate head to the brain. These ganglia are generated from the intermixing and coalescence of two distinct cell populations: cranial neural crest cells and placodal neurons. Trigeminal ganglion assembly requires the formation of cadherin-based adherens junctions within the neural crest cell and placodal neuron populations; however, the molecular composition of these adherens junctions is still unknown. Herein, we aimed to define the spatio-temporal expression pattern and function of Cadherin-7 during early chick trigeminal ganglion formation. Our data reveal that Cadherin-7 is expressed exclusively in migratory cranial neural crest cells and is absent from trigeminal neurons. Using molecular perturbation experiments, we demonstrate that modulation of Cadherin-7 in neural crest cells influences trigeminal ganglion assembly, including the organization of neural crest cells and placodal neurons within the ganglionic anlage. Moreover, alterations in Cadherin-7 levels lead to changes in the morphology of trigeminal neurons. Taken together, these findings provide additional insight into the role of cadherin-based adhesion in trigeminal ganglion formation, and, more broadly, the molecular mechanisms that orchestrate the cellular interactions essential for cranial gangliogenesis.

Keywords

Cadherin-7; neural crest; placodal neurons; trigeminal ganglion

1 | INTRODUCTION

The cranial ganglia of the peripheral nervous system perform crucial sensory functions, including somatosensation and innervation of specific organs such as the heart and lungs. The trigeminal ganglion (cranial nerve V) is responsible for the former, mediating sensations of pain, touch, and temperature in the face and innervating the sensory apparti of the muscles of the eye and upper and lower jaws. The collective intermixing and condensation of two embryonic cell populations, neural crest cells and neurogenic placode cells, is required to assemble the cranial ganglia (Breau & Schneider-Maunoury, 2015; Hamburger, 1961; Saint-Jeannet & Moody, 2014; Steventon, Mayor, & Streit, 2014). Neural crest cells arise from the dorsal region of the developing neural folds, undergo an epithelial-to-

Correspondence: Lisa A. Taneyhill, Department of Animal and Avian Sciences, University of Maryland, College Park, MD 20742. ltaney@umd.edu.

mesenchymal transition, and migrate to stereotypical destinations depending upon their axial level of origin and the molecular cues received from the extracellular environment (Bronner & Simoes-Costa, 2016; Duband, Dady, & Fleury, 2015; Gouignard, Andrieu, & Theveneau, 2018; Simoes-Costa & Bronner, 2015; Taneyhill & Schiffmacher, 2017). Neurogenic placode cells originate as paired epidermal thickenings at distinct rostral–caudal positions in the vertebrate head. These cells delaminate from the surface ectoderm (and while doing so begin differentiating) and then migrate through the cranial mesenchyme, where they will eventually coalesce with neural crest cells to form the cranial ganglia (Baker & Bronner-Fraser, 2001; Jidigam & Gunhaga, 2013; Smith, Fleenor, & Begbie, 2015; Steventon et al., 2014). Prior studies have highlighted the reciprocal nature of neural crest cell–placodal neuron interactions, providing a working hypothesis in which neural crest cells act as a scaffold to integrate all of the placodal neurons such that one ganglion forms, while placodal neurons, in turn, facilitate neural crest cell condensation (D'Amico-Martel & Noden, 1983; Hamburger, 1961; Shiau, Lwigale, Das, Wilson, & Bronner-Fraser, 2008). The interactions between neural crest cells and placodal neurons are also highly dynamic. Neural crest cells interact with epibranchial placode cells in the surface ectoderm, and later in development when these cells types are migrating and exhibit a "chase and run" behavior (Theveneau et al., 2013). Neural crest cells also form favorable pockets, or corridors, upon which placodal neurons prefer to migrate versus the less permissive mesoderm (Freter, Fleenor, Freter, Liu, & Begbie, 2013). As such, both transient and more stable intercellular interactions must occur between these two distinct cell types during their migration and coalescence to form a tightly adhered tissue.

Previous work has identified components of cadherin-based cellular adherens junctions, the levels of which must be tightly controlled to allow for proper intercellular interactions, during gangliogenesis. In the chick, placodal neurons express N-cadherin, and signaling between Slit1, secreted by neural crest cells, and Robo2, the Slit1 receptor on the surface of placodal neurons, regulates N-cadherin levels, likely through a posttranslational mechanism (Shiau et al., 2008; Shiau & Bronner-Fraser, 2009). Moreover, N-cadherin knockdown phenocopies depletion of Robo2, leading to more dispersed placodal neurons and, ultimately, defects in trigeminal ganglion condensation (Shiau & Bronner-Fraser, 2009). The presence of Cadherin-7 transcripts in the chick embryo was reported over 20 years ago using whole-mount in situ hybridization, which revealed *Cadherin*-7 expression in early migrating cranial neural crest cells (Hamburger-Hamilton stage 10 [HH10]) as well as in the forming trigeminal ganglion (HH18) (Nakagawa & Takeichi, 1995). Long-term overexpression of Cadherin-7 in chick trunk neural crest cells was shown to only abrogate migration of neural crest cells along the dorsolateral pathway (taken by melanocyte precursors) but did not inhibit neural crest cell differentiation (Nakagawa & Takeichi, 1998). The specific effect on melanocytes was ascribed to the timing at which the viral construct expressing Cadherin-7 achieved maximal levels (Nakagawa & Takeichi, 1998), and thus a functional role for Cadherin-7 in the neural crest was still not fully appreciated. More recent work revealed the presence of αN-catenin in migratory cranial neural crest cells, with perturbations in αN-catenin impacting trigeminal ganglion assembly, in part, through changes in the placodal neuron contribution to the ganglion and the level of Cadherin-7 in neural crest cells (Wu, Hooper, Han, & Taneyhill, 2014). No studies to date, however, have documented the spatio-

temporal expression pattern of Cadherin-7 protein in chick migratory cranial neural crest cells during early gangliogenesis, nor investigated the role of Cadherin-7 in neural crest cells that form the trigeminal ganglion.

To this end, we have undertaken studies to define the distribution and function of Cadherin-7 in migratory neural crest cells during early chick trigeminal gangliogenesis. Our data show that Cadherin-7 is expressed solely in migratory cranial neural crest cells as the trigeminal ganglion forms. To address Cadherin-7 function, we depleted and overexpressed Cadherin-7 in migratory neural crest cells and evaluated embryos for effects on trigeminal ganglion assembly. In each instance, we noted alterations in the distribution of neural crest cells and trigeminal neurons, along with abnormal trigeminal neuron morphology. Collectively, these results suggest that Cadherin-7 plays an important role in the migratory cranial neural crest cell population to permit correct trigeminal ganglion formation in the early chick embryo.

2 | RESULTS

2.1 | Cadherin-7 is expressed in migratory cranial neural crest cells contributing to the trigeminal ganglion

We documented the spatio-temporal expression pattern of Cadherin-7 protein throughout early stages of chick trigeminal gangliogenesis (HH12–17) using confocal microscopy, examining the forming ophthalmic lobe of the trigeminal ganglion (opV). In keeping with a previously published report on Cadherin-7 transcripts in the chick head (Nakagawa & Takeichi, 1995) and our prior study (Wu et al., 2014), we noted Cadherin-7 protein in migratory cranial neural crest cells (Figure 1a–d) identified by labeling with an antibody to HNK-1 (Bronner-Fraser, 1986) (Figure 1a′–d′) throughout all stages examined (HH13–16 shown, identical results observed for HH12 and 17). Cadherin-7 is primarily observed on the plasma membrane of neural crest cells, co-localizing with the cell surface HNK-1 neural crest cell marker (Figure 1a′–d′). Moreover, Cadherin-7 protein is observed in the neural tube (Figure 1a–d, *). In contrast, Cadherin-7 is not detected in the trigeminal placode precursors residing in the surface ectoderm nor in trigeminal neurons, here labeled with Annexin A6 (Figure 1a′–d′), as only placodal neurons express Annexin A6 at these stages of development (Shah & Taneyhill, 2015). To further demonstrate localization of Cadherin-7 to neural crest cells, we performed additional immunohistochemistry experiments on collected adjacent serial sections (due to antibody incompatibility issues), examining Cadherin-7, HNK-1 (neural crest cells), and Annexin A6 (placodal neurons) on one set of sections, and Pax3 (a marker of opV placode cells in the surface ectoderm or placodal neurons in the mesenchyme; [Stark, Sechrist, Bronner-Fraser, & Marcelle, 1997]), HNK-1, and Annexin A6 on the adjacent sections (Figure 2). These results show that placode cells and placodal neurons are Pax3-positive (with placodal neurons also Annexin A6-positive) but HNK-1-negative (Figure 2a–d′), while HNK-1-positive neural crest cells are immunoreactive for Cadherin-7 but not Annexin A6 (Figure 2e–h′). These data confirm our prior findings that Cadherin-7 is only expressed in migratory neural crest cells at these stages. Moreover, the cranial mesenchyme is devoid of Cadherin-7, as noted previously (Nakagawa & Takeichi, 1995). Our results also reveal that as opV forms over developmental time, migratory neural crest cells and placodal neurons condense together, forming a “tear

drop" shape that is apparent in transverse section, as noted previously (Shiau et al., 2008; Shiau & Bronner-Fraser, 2009). Thus, Cadherin-7 is expressed exclusively in migratory cranial neural crest cells throughout early trigeminal gangliogenesis.

2.2 | Reduced levels of Cadherin-7 alter trigeminal ganglion assembly through effects on neural crest cells and placodal neurons

To assess the functional role of Cadherin-7 in neural crest cells contributing to the trigeminal ganglion, we performed morpholino (MO)-mediated knockdown of *Cadherin*-7 using a translation-blocking MO that targets the Cadherin-7 5′ UTR and initial coding region (see Section 4). As a control, we designed a 5 bp mismatch Cadherin-7 MO that does not block *Cadherin*-7 translation. This MO is specific to Cadherin-7, as demonstrated by a search of the chick genome, which revealed a lack of targeting of the MO to any other *cadherin* (or other) transcript. Furthermore, we compared the sequence surrounding the start site of translation in *Cadherin*-7 that is targeted by the Cadherin-7 MO with other known Cadherin family members expressed in premigratory and migratory cranial neural crest cells (*E-cadherin*, *N-cadherin*, *Cadherin-6B, Cadherin-11*), as well as other *cadherins* expressed in the neural tube or the region of the forming trigeminal ganglion (based upon expression patterns in the chick GEISHA in situ hybridization database). Our results once again indicate that the Cadherin-7 MO is only targeting *Cadherin*-7 (Figure 3a).

To examine the efficacy of the Cadherin-7 MO, we electroporated either the Cadherin-7 or control MO into migratory neural crest cells and performed immunoblotting for Cadherin-7 protein on lysates prepared from electroporated, dissected trigeminal ganglia, as in (Shah et al., 2017). We noted an approximate 50% reduction in Cadherin-7 protein levels in tissue possessing the Cadherin-7 MO versus the control MO (Figure 3b,c, n = 2). Taken together with our evaluation of the chick genome described above, the Cadherin-7 MO is targeting exclusively *Cadherin-7*, and we next set out to use this MO to ascertain the function of Cadherin-7 in trigeminal ganglion assembly.

To this end, we determined whether knockdown of Cadherin-7 affects neural crest cells and placodal neurons contributing to the ophthalmic lobe of the trigeminal ganglion. Premigratory cranial neural crest cells were unilaterally electroporated with the Cadherin-7 or control MO, and embryos were allowed to grow to HH15–16 followed by immunohistochemistry on cranial transverse sections using molecular markers to label neural crest cells (HNK-1) and placodal neurons (Tubb3), the latter of which only labels placode cell-derived neurons at this stage of development (Moody, Quigg, & Frankfurter, 1989; Shiau et al., 2008), as neural crest cells differentiate much later (D'Amico-Martel & Noden, 1980; Steventon et al., 2014). Introduction of the control MO (Figure 4a) into migratory neural crest cells did not affect the distribution of neural crest cells and trigeminal neurons, as assessed by HNK-1 (Figure 4b) and Tubb3 (Figure 4c) immunohistochemistry, nor their ability to coalesce together (Figure 4d, d′). Depletion of Cadherin-7 through introduction of the Cadherin-7 MO (Figure 4e), however, impacted both the neural crest cell and trigeminal neuron populations in the ganglionic anlage. Neural crest cells appear more dispersed and do not entirely surround placodal neurons (Figure 4f, h′; n = 13/13 embryos, all embryos examined were HH15 or 16); compare to Figure 4b, d′; n = 6/6 embryos, all

embryos analyzed were HH15 or 16). Interestingly, trigeminal neurons were also affected, with these cells possessing fewer neurites and thus appearing round instead of bipolar (Figure 4g, h′, n = 13/13 embryos, all embryos examined were HH15 or 16) compared to the morphology adopted by trigeminal neurons in control MO-treated embryos (Figure 4c, d′, n = 5/5 embryos, all embryos analyzed were HH15 or 16). In addition, trigeminal neurons tended to aggregate together in small clusters or groups (Figure 4g, h′).

To rule out potential indirect effects on neural crest cells that could be causing these phenotypes during ganglion assembly, such as changes in cell proliferation or cell death, we next performed phospho-histone H3 (PHH3) immunohistochemistry as well as a TUNEL assay, respectively. Upon counting PHH3-or TUNEL-positive cells and comparing the contralateral control and MO-treated sides, we noted no statistically significant difference in either cell proliferation (Figure 5a–d, all embryos for PHH3 analyses were HH15 or 16, with four embryos examined for each treatment, all values reported as mean ± SEM; 24 ± 1 PHH3-positive cells for the control MO-treated side, 23 ± 1 PHH3-positive cells for the contralateral side, unpaired Student's t test, $p = .84$; 24 ± 1 PHH3-positive cells for the Cadherin-7 MO-treated side, 25 ± 1 PHH3-positive cells for the contralateral side, unpaired Student's t test, $p = .71$) or cell death (Figure 5e–h, all embryos for TUNEL analyses were HH15 or 16, all values reported as mean ± SEM; 31 ± 2 TUNEL-positive cells for the control MO-treated side, 30 ± 3 TUNEL-positive cells for the contralateral side, unpaired Student's t test, p = .63, n = 3 embryos; 24 ± 2 TUNEL-positive cells for the Cadherin-7 MO-treated side, 23 ± 2 TUNEL-positive cells for the contralateral side, unpaired Student's t test, $p = .71$, n = 4 embryos). As such, the overall organization of the trigeminal ganglion appeared abnormal upon Cadherin-7 knockdown in neural crest cells due to effects on both migratory neural crest cells and placodal neurons unrelated to changes in cell proliferation or cell death.

Given the observed phenotypes in tissue sections, we next examined the distribution of neural crest cells and placodal neurons within the context of the entire trigeminal ganglion by performing whole-mount immunohistochemistry for HNK-1 and Tubb3, respectively. Lateral views of whole embryo heads at HH15–16 obtained by confocal microscopy revealed the normal distribution of neural crest cells and placodal neurons within the trigeminal ganglion in the presence of the control MO (Figure 6a–d, n = 10/10 embryos, all embryos analyzed were HH15 or 16). In these images, placodal neurons condense with migratory neural crest cells to generate the stereotypical bilobed or semilunar structure of the trigeminal ganglion that is revealed through the Tubb3-positive immunoreactivity of the placodal neurons when viewed in whole embryos (Figure 6c, d) (Shiau et al., 2008; Shiau & Bronner-Fraser, 2009). This structure of the trigeminal ganglion is altered, however, upon MO-mediated knockdown of Cadherin-7 (Figure 6e–h, n = 11/13 embryos, all embryos are HH15 or 16). From these experiments, it is apparent that Cadherin-7-depleted neural crest cells still localized to the anlage, allowing them to intermingle with trigeminal neurons (compare Figure 6f to Figure 6b). Even with this seemingly correct localization, though, the ganglion appears truncated, particularly the ophthalmic lobe, with Tubb3-positive trigeminal neurons less condensed with themselves (and with neural crest cells) in both lobes of the ganglion (compare Figure 6g, h, to Figure 6c, d). Collectively, these data provide evidence for a role for Cadherin-7 in neural crest cells during trigeminal ganglion assembly.

2.3 | Overexpression of Cadherin-7 negatively affects trigeminal ganglion assembly by impacting both neural crest cells and placodal neurons

To further elucidate the function of Cadherin-7 in migratory cranial neural crest cells, we overexpressed Cadherin-7 and evaluated effects on the neural crest and placodal neuron populations forming the trigeminal ganglion. Cadherin-7 protein levels were increased by 200% over control, as assessed by immunoblotting for Cadherin-7 in lysates prepared from electroporated, dissected trigeminal ganglia possessing the control vector (pCIG) versus the Cadherin-7 expression construct (pCIG-Cad7, contains an IRES-GFP cassette to label electroporated cells; see Section 4 for details) (Figure 7, n = 2). Next, we evaluated how augmented Cadherin-7 protein levels in neural crest cells affect trigeminal ganglion formation. To this end, we performed similar neural crest cell electroporation experiments and analyzed tissue sections (Figure 8) and whole embryo heads (Figure 10) for changes in neural crest cells and/or placodal neurons contributing to the trigeminal ganglion. In the presence of the control pCIG vector (Figure 8a), we noted no alterations in migratory neural crest cells (Figure 8b, n = 8/8 embryos, all embryos examined were HH15 or 16) or placodal neurons (Figure 8c, n = 8/8 embryos, all embryos analyzed were HH15 or 16). These results indicate that the trigeminal ganglion assembled normally (Figure 8d) and that the electroporation technique did not affect its formation. Cadherin-7 overexpression in neural crest cells, however, negatively impacted trigeminal ganglion assembly. Neural crest cells expressing increased levels of Cadherin-7 (Figure 8e, f) are present within the ganglionic anlage and still surround placodal neurons; however, their interactions with placodal neurons are altered, leading to the presence of two separate foci consisting of Tubb3-positive placodal neurons (Figure 8g, h, h′; n = 13/15 embryos, all embryos examined were HH15 or 16; compare to Figure 8c,d,d′). The morphology of placodal neurons was also affected, with neurons appearing, in some instances, more round as opposed to the bipolar shape that these neurons normally possess, and often look misshapen (Figure 8g, h′; n = 21/22 embryos, all embryos examined were HH15 or 16; compare to Figure 8c, d′). Finally, the “tear drop” shape of the ganglion often observed at this developmental stage in section (Figure 8d; see Figures 1 and 4b) (Shiau et al., 2008; Shiau & Bronner-Fraser, 2009) is also not apparent after Cadherin-7 overexpression (Figure 8h).

To confirm that the observed phenotypes were not due to nonspecific effects on cell proliferation or death, we conducted phospho-histone H3 immunohistochemistry and a TUNEL assay, respectively. We noted no statistically significant change in either cell proliferation (Figure 9a–d, all embryos for PHH3 analyses were HH15 or 16, with four embryos examined for each treatment, all values reported as mean ± SEM; 31 ± 1 PHH3-positive cells for the pCIG control-treated side; 30 ± 1 PHH3-positive cells for the contralateral side, unpaired Student’s t test, $p = .82$; 26 ± 1 PHH3-positive cells for the pCIG-Cad7-treated side, 26 ± 1 PHH3-positive cells for the contralateral side, unpaired Student’s t test, $p = .72$) or cell death (Figure 9e–h, all embryos for TUNEL analyses were HH15 or 16, all values reported as mean ± SEM; 22 ± 2 TUNEL-positive cells for the pCIG control-treated side, 21 ± 2 TUNEL-positive cells for the contralateral side, unpaired Student’s t test, $p = .71$, $n = 3$ embryos; 31 ± 2 TUNEL-positive cells for the pCIG-Cad7-treated side, 30 ± 3 TUNEL-positive cells for the contralateral side, unpaired Student’s t test, $p = .78$, $n = 4$ embryos). Collectively, these results further confirm that Cadherin-7

expression in neural crest cells is important for appropriate trigeminal ganglion assembly and that the noted phenotypes are not caused by changes in cell proliferation or cell death.

Given these results in tissue sections, we then analyzed whole embryo heads from HH15–16 embryos by confocal microscopy following immunostaining for HNK-1 and Tubb3, as we had done previously with our MO-electroporated embryos (Figure 10). Introduction of the pCIG control vector (Figure 10a) into migratory neural crest cells revealed no effects on neural crest cell–placodal neuron interactions and, ultimately, trigeminal gangliogenesis (Figure 10a–d, $n = 7/7$ embryos, all embryos examined were HH15 or 16), as exemplified by Tubb3 immunoreactivity and the formation of a ganglion possessing a bilobed structure (Figure 10c). Cadherin-7 overexpression, however, disrupted trigeminal ganglion assembly, as evidenced by the presence of a disorganized ganglion with the gross morphology appearing less bilobed than observed in control embryos (Figure 10e–h, $n = 7/7$ embryos, all embryos analyzed were HH15 or 16). While HNK-1-positive neural crest cells migrated and localized to the ganglionic anlage, their distribution was noticeably different than that observed with the pCIG control vector, with neural crest cells aggregating together (compare Figure 10e,f to Figure 10a,b). While trigeminal placodal neurons do intermix with the aberrantly localized neural crest cells, this causes them to be less compact in appearance (compare Figure 10c,d to Figure 10g,h). Taken together with our knockdown data, these findings reveal the importance of controlling Cadherin-7 levels in neural crest cells, and ultimately proper neural crest cell-placodal neuron interactions, during trigeminal gangliogenesis.

3 | DISCUSSION

3.1 | Migratory cranial neural crest cells contributing to the trigeminal ganglion express Cadherin-7 throughout early gangliogenesis

The assembly of the cranial trigeminal ganglion requires the coalescence of distinct migratory cell populations, neural crest cells and placodal neurons, which are derived from different tissues (Breau & Schneider-Maunoury, 2015; D'Amico-Martel & Noden, 1983; Hamburger, 1961; Saint-Jeannet & Moody, 2014; Steventon et al., 2014). Cranial neural crest cells leave the neural ectoderm through an epithelial-to-mesenchymal transition and become highly invasive, migrating to the ganglionic anlage (Bronner & Simoes-Costa, 2016; Duband et al., 2015; Gouignard et al., 2018; Simoes-Costa & Bronner, 2015; Taneyhill & Schiffmacher, 2017). During their migration, cranial neural crest cells interact with placode cells within the surface ectoderm prior to their delamination as well as with placodal neurons that have already delaminated from the surface ectoderm and differentiated (Breau & Schneider-Maunoury, 2015; Theveneau et al., 2013). These interactions must be productive to allow for cell-cell adhesion and the eventual correct formation of the cranial ganglia. A prior study noted that N-cadherin expression in trigeminal placodal neurons is critical for mediating proper trigeminal ganglion condensation (Shiau & Bronner-Fraser, 2009), but molecules important in cranial neural crest cells had yet to be identified. Here, we investigated the role of Cadherin-7 in neural crest cells during trigeminal ganglion assembly. We first documented the spatio-temporal expression pattern of Cadherin-7 protein during early stages of trigeminal gangliogenesis. We observed Cadherin-7 protein exclusively in

migratory cranial neural crest cells as early as HH12 (not shown), with no detectable protein present in trigeminal placodal precursors or their neuronal derivatives (Figures 1 and 2). These results now expand upon our prior publication examining the expression and function of adherens junction components in neural crest cells during trigeminal gangliogenesis (αN-catenin in neural crest cells [Wu et al., 2014]). Taken together with these other publications, our new data establish the importance of cadherin-based adhesion during trigeminal ganglion formation, with distinct cadherins expressed in the neural crest cell (Cadherin-7) and placodal neuron (N-cadherin) populations.

3.2 | Trigeminal ganglion formation relies upon proper levels of Cadherin-7 in migratory cranial neural crest cells

To explore a function for Cadherin-7 in the cranial neural crest cell population, we undertook molecular perturbation assays to reduce (MO) or elevate (overexpression) Cadherin-7 levels in migratory neural crest cells. MO-mediated knockdown achieved a 50% reduction in Cadherin-7 protein, as assessed by immunoblotting, which, in turn, impacted trigeminal ganglion assembly (Figures 4 and 6). Migratory neural crest cells depleted for Cadherin-7 still migrated to the ganglionic anlage, but their distribution was altered compared to neural crest cells in control MO-treated embryos. Moreover, trigeminal neurons were also affected at the level of both their morphology and distribution. In many instances, these neurons remained round and did not elaborate neurites characteristic of mature neurons, although they did express Tubb3, indicative of their molecular maturation. This alteration to trigeminal neuron morphology mirrors that observed upon loss of Annexin A6 (Shah et al., 2017) or N-cadherin (Shiau & Bronner-Fraser, 2009) in placodal neurons. Effects on trigeminal neurons upon changes to molecules in neural crest cells are not without precedent, as noted previously upon depletion of αN-catenin in neural crest cells, which changes the distribution of trigeminal neurons (noted in transverse sections) and affects gross ganglion formation (observed in whole-mount), shown by immunohistochemistry for Islet-1 and Tubb3, respectively (Wu et al., 2014). Moreover, modulation of N-cadherin levels in placodal neurons also affects neural crest cells contributing to the trigeminal ganglion (Shiau & Bronner-Fraser, 2009). Such cell nonautonomous effects are not surprising given that both N-cadherin and Cadherin-7 are transmembrane cell adhesion molecules. Overall, trigeminal ganglion morphology also appeared abnormal and was apparent in lateral whole-mount views of embryo heads following Cadherin-7 MO electroporation. In these experiments, Cadherin-7-depleted embryos possessed truncated ophthalmic lobes within their trigeminal ganglia, with trigeminal neurons appearing more dispersed. Collectively, our section and whole embryo results indicate that decreased levels of Cadherin-7 impact overall trigeminal ganglion assembly, likely at the level of both the neural crest cells and placodal neurons.

We next performed the converse experiment in which we overexpressed Cadherin-7 in migratory cranial neural crest cells. With a 200% increase in neural crest Cadherin-7 levels, as evaluated by immunoblotting, we noted, once again, defective trigeminal ganglion assembly, in both section and whole embryo images (Figures 8 and 10). In these experiments, neural crest cells still migrate to the anlage in the presence of elevated levels of Cadherin-7; however, their distribution is aberrant, with neural crest cells aggregating

together. Consequently, the location and morphology of trigeminal neurons is negatively impacted. These neurons, while normally possessing a bipolar morphology and surrounded by neural crest cells in control embryos, are often times clustered together (but still surrounded by neural crest cells) and exhibit an aberrant shape upon overexpression of Cadherin-7 in neural crest cells. These changes in the distribution of neural crest cells and placodal neurons are also noted in images of the forming trigeminal ganglion in whole embryo heads. Similar to our results in which Cadherin-7 levels are reduced, elevated levels of Cadherin-7 led to a noticeable change in the distribution and organization of neural crest cells and trigeminal neurons. Taken together, our knockdown and overexpression results establish a new role for Cadherin-7 in cranial neural crest cells during trigeminal ganglion assembly.

3.3 | Neural crest cell–placodal neuron adhesion plays a key role in trigeminal gangliogenesis

Our data indicate that neural crest cells possessing reduced or elevated levels of Cadherin-7 negatively affects trigeminal ganglion assembly, with defects noted in the distribution of neural crest cells and placodal neurons within the ganglionic anlage. Notably, these results cannot be attributed to changes in cell proliferation or cell death within the forming trigeminal ganglion (Figures 5 and 9). Therefore, our findings further underscore that cell adhesion molecules expressed by neural crest cells and placodal neurons play key roles in regulating ganglion formation. Results published almost a decade ago described the importance of N-cadherin in placodal neurons, including its function in mediating placodal neuron aggregation (Shiau & Bronner-Fraser, 2009). In these experiments, MO-mediated knockdown of N-cadherin in trigeminal placode precursor cells impeded placodal neuron aggregation later in development. Placodal neurons appear more dispersed (evident in section and whole embryo images), much like what we observe for placodal neurons upon Cadherin-7 knockdown in neural crest cells. Moreover, N-cadherin overexpression also resulted in aberrant trigeminal ganglion assembly due to the presence of atypical clusters of placodal neurons, along with an apparent loss of placodal neurons (all noted in whole embryo images). This latter result is intriguing given the comparable placodal neuron phenotypes that we observe in whole embryo heads upon Cadherin-7 overexpression in neural crest cells. Unfortunately, effects on the cranial neural crest cell population upon N-cadherin perturbation were not examined in this earlier report. Collectively, our findings reveal that alterations in the levels of cadherins in cranial neural crest cells and trigeminal neurons can severely impact proper ganglion assembly.

Given the observed effect on trigeminal neurons upon changes in neural crest cell Cadherin-7 levels, it is possible neural crest cell corridors do not form entirely correctly in embryos possessing neural crest cells with increased or decreased Cadherin-7 levels. These corridors provide a more permissive substrate (vs. the mesoderm) upon which placodal neurons migrate during the formation of the cranial ganglia (Freter et al., 2013). We hypothesize that this could be one mechanism by which changes in neural crest cells affect the distribution and morphology of placodal neurons. Furthermore, elevated levels of Cadherin-7 in neural crest cells could promote increased adhesion between neural crest cells and hinder the ability of these cells to form interactions with placodal neurons. Support for

this hypothesis stems from our whole-mount immunohistochemistry images, which show aggregates of neural crest cells after Cadherin-7 overexpression (Figure 10). Future studies will be necessary to determine whether parameters associated with neural crest cell adhesion and migration (e.g., velocity, directionality) are impacted upon changes in Cadherin-7. In addition, we surmise that alterations in Cadherin-7 levels in neural crest cells could influence N-cadherin distribution and/or levels in placodal neurons, although we have been unable to detect any qualitative changes in N-cadherin by immunohistochemistry upon Cadherin-7 depletion or overexpression. Based on our findings that cadherins are under a high degree of posttranslational regulation (e.g., proteolysis: [Schiffmacher, Padmanabhan, Jhingory, & Taneyhill, 2014]), however, this does not preclude potential changes in placodal neuron adhesion, which will be borne out in future experiments.

The use of different cadherins, and specifically Cadherin-7 and N-cadherin, to achieve patterning has been described as various tissues form in the chick, including the retina (Wohrn, Puelles, Nakagawa, Takeichi, & Redies, 1998), cochlea (Luo, Wang, Lin, & Redies, 2007), and tectum (Wohrn, Nakagawa, Ast, Takeichi, & Redies, 1999). Although these studies were carried out at much later embryonic stages (>E5), the findings still reveal the importance of Cadherin-7 and N-cadherin expression in different cell types to effectively pattern these tissues. General heterophilic (i.e., non-like) cadherin interactions between distinct types of cells have been reported previously, during both normal development (e.g., the endoderm [Straub et al., 2011]; synaptic potentiation within the hippocampus [Basu et al., 2017]) and during disease (e.g., cancer cell invasion [Labernadie et al., 2017]). Future studies will be geared at understanding the role of Cadherin-7 and N-cadherin in regulating intercellular interactions within the assembling trigeminal ganglion.

In summary, our data provide additional evidence for the importance of properly regulating levels of cadherin proteins during trigeminal ganglion assembly. These findings point to a new role for Cadherin-7 in controlling the formation of the trigeminal ganglion. Altogether, these results further underscore the importance of cadherin-based intercellular interactions that are requisite for cranial gangliogenesis and proper patterning of the vertebrate peripheral nervous system.

4 | MATERIALS AND METHODS

4.1 | Chick embryos

Fertilized chicken eggs (*Gallus gallus*) were obtained from Centurion Poultry (Lexington, GA) and Moyer's Chicks, Inc. (Quakertown, PA), and incubated at 37 °C in humidified incubators (EggCartons.com, Manchaug, MA). Embryos were staged by the Hamburger-Hamilton (HH) staging method (Hamburger & Hamilton, 1992) or by counting the number of somite pairs (somite stage, ss).

4.2 | Cadherin-7 morpholinos and expression constructs

A 3′ lissamine-labeled antisense translation-blocking Cadherin-7 morpholino (MO, 5-ACTCCACTTTGCCCAACTTCATCTT-3′), or a 5-base pair mismatch Cadherin-7 control MO (5′-AaTCCAaTTTGCCaAAaTT-CATaTT-3′) (start codon underlined, mismatches

shown in lowercase), was designed to target the *Cadherin*-7 transcript according to the manufacturer's criteria (GeneTools, LLC, Philomath, OR). Both MOs were used at a concentration of 500 μM, as described previously (Wu et al., 2014). Based upon the recommendations outlined by Drs. Moulton and Vincent (GeneTools, LLC), we searched the chicken genome using the BLAST function (and the sequence in *Cadherin-7* that is complementary to the Cadherin-7 MO) to identify other transcripts that the MO might potentially target for translational knockdown. However, these transcripts will only be targeted by the MO if they fit the following criteria: (a) the MO is complementary to a putative candidate transcript 5′ UTR or within the first 25 nucleotides of the coding sequence (to sterically block the translation initiation complex); (b) the MO is targeted to the sense strand; (c) the MO and transcript have a minimum 14 nucleotide consecutive match; and (d) the MO acts on a transcript expressed in the tissue of interest (neural crest). In our search, we found no cadherin, or other genes (besides *Cadherin-7*), that fulfilled these criteria. A DNA construct designed for Cadherin-7 overexpression (pCIG-Cad7), which contains an IRES-GFP cassette to label electroporated cells, was a kind gift from Dr. Marianne Bronner (California Institute of Technology). The control pCIG vector (just the IRES-GFP cassette), or pCIG-Cad7, was used at a concentration of 2.5 μg/μl as in (Wu et al., 2014).

4.3 | In ovo unilateral electroporations

Unilateral electroporation of the early chick neural tube was conducted to target migratory neural crest cells in the trigeminal ganglionic anlage, as carried out previously (Wu et al., 2014). Briefly, MOs or expression constructs were introduced into premigratory midbrain neural crest cells in developing 3–4 somite stage (3–4ss) chick embryos using fine glass needles and filling of the chick neural tube. Platinum electrodes were placed on either side of the embryo, and two 25 V, 25 ms electric pulses were applied across the embryo. Eggs were re-sealed with tape and parafilm, re-incubated for 12 hr, and then imaged in ovo around HH12 (prior to embryo turning) using a Zeiss Discovery. V8 stereomicroscope in order to evaluate presence of MOs or expression constructs. After imaging, eggs containing MO- or expression construct-positive embryos were re-sealed and re-incubated for the desired time period prior to harvesting for further experimentation.

4.4 | Immunoblotting

Chick embryo neural crest cells were electroporated as described above with either MO or expression constructs. Approximately 35 hr post-electroporation, trigeminal ganglia were excised, pooled, pelleted, flash-frozen in liquid nitrogen, and stored at −80 °C until required for immunoblot analysis. Protein lysis, extraction, fraction, and immunoblotting were performed as described previously (Schiffmacher et al., 2018; Shah et al., 2017). Briefly, pellets were thawed on ice and lysed in lysis buffer (50 mM Tris pH 8.0, 150 mM NaCl, 1% IGEPAL CA-630) supplemented with cOmplete protease inhibitor cocktail (Roche, Basel, Switzerland) and 1 mM PMSF for 30 min at 4 °C with periodic mixing. Soluble fractions were collected following centrifugation (g) at maximum for 15 min at 4 °C, and protein concentration was quantified by Bradford assay (Thermo Fisher Scientific, Rockford, IL). Equivalent amounts of protein per sample were processed by SDS-PAGE (10% Mini-Protean TGX gel, BioRad #456–1034) and then transferred to 0.45 μm BioTrace PVDF

membrane (Pall, Port Washington, NY) via the iBlot transfer stack system (iBlot 2 Dry Blotting system, Life Technology # IB21001) according to the manufacturer's guidelines. Primary antibodies used for immunoblotting were Cadherin-7 (Developmental Studies Hybridoma Bank [DSHB] (Iowa City, IA), clone CCD7–1, 1:150) and β-actin (Santa Cruz Biotechnology sc-47,778, 1:1,000). Immunoblot images for figures were gamma-modified and processed using Adobe Photoshop CC 2015.5 (Adobe Systems, San Jose, CA). Immunoblot band volumes (intensities) were calculated from unmodified immunoblot images using Image Lab software (Bio-Rad, Hercules, CA), and relative protein levels were determined by normalizing the volumes of Cadherin-7 bands to those of β-actin. Differences in the amount of Cadherin-7 were assessed by comparing normalized ratios between either control MO- and Cadherin-7 MO-treated samples, or pCIG- and pCIG-Cad7-treated samples, with the control MO- and pCIG-treated samples set to one.

4.5 | Immunohistochemistry and TUNEL assay

Embryos were collected at the designated stages for wildtype or postelectroporation immunohistochemistry. Detection of various proteins was performed in whole-mount following overnight fixation in 4% PFA, or on 14 μm transverse sections following 4% PFA fixation, gelatin embedding, and cryostat sectioning as described previously (Shah et al., 2017; Wu et al., 2014). All primary and secondary antibodies were diluted in 1× phosphate-buffered saline + 0.1% Triton X-100 (PBSTX) + 5% sheep serum. The following antibodies and dilutions were used for immunohistochemistry: Cadherin-7 (DSHB, clone CCD7–1, 1:100); N-cadherin (DSHB, clone MNCD2, 1:200); HNK-1 (DSHB, clone 3H5, 1:100); Tubb3 (Abcam 2G10, ab78078, 1:500 (Cambridge, MA)); Annexin A6 (Abnova, PAB18085, 1:100 (Taipei City, Taiwan)); Pax3 (DSHB, clone C2, 1:100), GFP (Abcam, ab6662, 1:300); and phospho-histone H3 (Millipore Sigma, 1:200 (St. Louis, MO, USA)). The following secondary antibodies were used at 1:200–1:500 dilutions: goat anti-mouse IgG (Life Technologies, Cadherin-7); goat anti-rat IgG (Life Technologies, N-cadherin (Carlsbad, CA, USA)); goat anti-mouse IgM (Life Technologies, HNK-1); goat anti-mouse IgG_{2a} (Southern Biotech, Tubb3 or Pax3 (Birmingham, AL, USA)); and goat anti-rabbit IgG (Life Technologies, Annexin A6 and phospho-histone H3). Sections were stained with 4′,6-diamidino-2-phenylindole (DAPI) to mark cell nuclei using DAPI-containing mounting media (Fluoromount G, Southern Biotech). A TUNEL assay (Roche, TMR red and fluorescein (Basel, Switzerland)) was performed on 4% PFA-fixed, cryopreserved sections to detect apoptotic cells as described previously (Shah et al., 2017; Wu et al., 2014) followed by mounting of slides with DAPI-containing media as outlined above.

4.6 | Confocal imaging

For all experiments, images of at least five serial transverse sections through a minimum of eight embryos (unless indicated otherwise), or of a minimum of seven embryo heads (unless indicated otherwise), were acquired with the LSM Zeiss 800 confocal microscope with Airyscan detection (Carl Zeiss Microscopy, Thornwood, NY) at ×20 or ×5 magnification, respectively. To acquire images of the trigeminal ganglion in the chick head, embryos were mounted on viewing slides, and a lateral view of the chick head containing the forming trigeminal ganglion was captured. Where possible, the laser power, gain, and offset were kept consistent for the different channels throughout all experiments. Image processing was

conducted with the Zen Blue software (Carl Zeiss Microscopy) and Adobe Photoshop CC 2015.5.

4.7 | Quantification and statistical analysis

To analyze the effect of Cadherin-7 knockdown or overexpression on cell proliferation and cell death, phospho-histone H3- and TUNEL-positive cells were counted following immunohistochemistry (or TUNEL assay) using the Adobe Photoshop count tool. Cells were counted within the region of the forming trigeminal ganglion in a minimum of five serial transverse sections taken from at least three electroporated embryos per treatment, on both the experimentally treated and contralateral control sides of the section. Cell counts were then compared within embryo treatment groups. All results are reported as the average number of phospho-histone H3- or TUNEL-positive cells, plus or minus the standard error of the mean, and were analyzed with an unpaired Student's t test to establish statistical significance as carried out previously (Shah et al., 2017; Wu et al., 2014).

ACKNOWLEDGMENTS

We thank Ms. Vinona Muralidaran, Ms. Reethika Maddineni, and Ms. Julie Ren for excellent technical assistance. We also thank Dr. Marianne Bronner (California Institute of Technology) for the Cadherin-7 expression construct (pCIG-Cad7) and Dr. Celia Shiau (University of North Carolina) for useful discussions on trigeminal ganglion formation. The authors declare no competing financial interests. This work was supported by a grant to L.A.T. (NIH R01DE024217).

Funding information National Institute of Dental and Craniofacial Research, Grant/Award Number: R01 DE024217; NIH, Grant/Award Number: R01DE024217

REFERENCES

Baker CV, & Bronner-Fraser M (2001). Vertebrate cranial placodes I. Embryonic induction. Developmental Biology, 232, 1–61. [PubMed: 11254347]

Basu R, Duan X, Taylor MR, Martin EA, Muralidhar S, Wang Y, … Williams ME (2017). Heterophilic type II Cadherins are required for high-magnitude synaptic potentiation in the hippocampus. Neuron, 96, 160–176e8. [PubMed: 28957665]

Breau MA, & Schneider-Maunoury S (2015). Cranial placodes: Models for exploring the multi-facets of cell adhesion in epithelial rearrangement, collective migration and neuronal movements. Developmental Biology, 401, 25–36. [PubMed: 25541234]

Bronner ME, & Simoes-Costa M (2016). The neural crest migrating into the twenty-first century. Current Topics in Developmental Biology, 116, 115–134. [PubMed: 26970616]

Bronner-Fraser M (1986). Analysis of the early stages of trunk neural crest migration in avian embryos using monoclonal antibody HNK-1. Developmental Biology, 115, 44–55. [PubMed: 3516760]

D'Amico-Martel A, & Noden DM (1980). An autoradiographic analysis of the development of the chick trigeminal ganglion. Journal of Embryology and Experimental Morphology, 55, 167–182. [PubMed: 6966308]

D'Amico-Martel A, & Noden DM (1983). Contributions of placodal and neural crest cells to avian cranial peripheral ganglia. The American Journal of Anatomy, 166, 445–468. [PubMed: 6858941]

Duband JL, Dady A, & Fleury V (2015). Resolving time and space constraints during neural crest formation and delamination. Current Topics in Developmental Biology, 111, 27–67. [PubMed: 25662257]

Freter S, Fleenor SJ, Freter R, Liu KJ, & Begbie J (2013). Cranial neural crest cells form corridors prefiguring sensory neuroblast migration. Development, 140, 3595–3600. [PubMed: 23942515]

Gouignard N, Andrieu C, & Theveneau E (2018). Neural crest delamination and migration: Looking forward to the next 150 years. Genesis, 56(6–7), e23107. [PubMed: 29675839]

Hamburger V (1961). Experimental analysis of the dual origin of the trigeminal ganglion in the chick embryo. The Journal of Experimental Zoology, 148, 91–123. [PubMed: 13904079]

Hamburger V, & Hamilton HL (1992). A series of normal stages in the development of the chick embryo. 1951. Developmental Dynamics, 195(4), 231–272. [PubMed: 1304821]

Jidigam VK, & Gunhaga L (2013). Development of cranial placodes: Insights from studies in chick. Development, Growth & Differentiation, 55, 79–95.

Labernadie A, Kato T, Brugues A, Serra-Picamal X, Derzsi S, Arwert E, … Trepat X (2017). A mechanically active heterotypic E-cadherin/N-cadherin adhesion enables fibroblasts to drive cancer cell invasion. Nature Cell Biology, 19, 224–237. [PubMed: 28218910]

Luo J, Wang H, Lin J, & Redies C (2007). Cadherin expression in the developing chicken cochlea. Developmental Dynamics, 236, 2331–2337. [PubMed: 17654718]

Moody SA, Quigg MS, & Frankfurter A (1989). Development of the peripheral trigeminal system in the chick revealed by an isotypespecific anti-beta-tubulin monoclonal antibody. The Journal of Comparative Neurology, 279, 567–580. [PubMed: 2918088]

Nakagawa S, & Takeichi M (1995). Neural crest cell-cell adhesion controlled by sequential and subpopulation-specific expression of novel cadherins. Development, 121, 1321–1332. [PubMed: 7540531]

Nakagawa S, & Takeichi M (1998). Neural crest emigration from the neural tube depends on regulated cadherin expression. Development, 125, 2963–2971. [PubMed: 9655818]

Saint-Jeannet JP, & Moody SA (2014). Establishing the pre-placodal region and breaking it into placodes with distinct identities. Developmental Biology, 389, 13–27. [PubMed: 24576539]

Schiffmacher AT, Adomako-Ankomah A, Xie V, & Taneyhill LA (2018). Cadherin-6B proteolytic N-terminal fragments promote chick cranial neural crest cell delamination by regulating extracellular matrix degradation. Developmental Biology, S0012-1606(17), 30609–7. https://doi.org/10.1016/j.ydbio.2018.06.018

Schiffmacher AT, Padmanabhan R, Jhingory S, & Taneyhill LA (2014). Cadherin-6B is proteolytically processed during epithelial-to-mesenchymal transitions of the cranial neural crest. Molecular Biology of the Cell, 25, 41–54. [PubMed: 24196837]

Shah A, Schiffmacher AT, & Taneyhill LA (2017). Annexin A6 controls neuronal membrane dynamics throughout chick cranial sensory gangliogenesis. Developmental Biology, 425, 85–99. [PubMed: 28315296]

Shah A, & Taneyhill LA (2015). Differential expression pattern of Annexin A6 in chick neural crest and placode cells during cranial gangliogenesis. Gene Expression Patterns, 18, 21–28. [PubMed: 25976293]

Shiau C, Lwigale P, Das R, Wilson S, & Bronner-Fraser M (2008). Robo2-Slit1 dependent cell-cell interactions mediate assembly of the trigeminal ganglion. Nature Neuroscience, 11, 269–276. [PubMed: 18278043]

Shiau CE, & Bronner-Fraser M (2009). N-cadherin acts in concert with Slit1-Robo2 signaling in regulating aggregation of placode-derived cranial sensory neurons. Development, 136, 4155–4164. [PubMed: 19934013]

Simoes-Costa M, & Bronner ME (2015). Establishing neural crest identity: A gene regulatory recipe. Development, 142, 242–257. [PubMed: 25564621]

Smith AC, Fleenor SJ, & Begbie J (2015). Changes in gene expression and cell shape characterise stages of epibranchial placode-derived neuron maturation in the chick. Journal of Anatomy, 227, 89–102. [PubMed: 26076761]

Stark MR, Sechrist J, Bronner-Fraser M, & Marcelle C (1997). Neural tube-ectoderm interactions are required for trigeminal placode formation. Development, 124, 4287–4295. [PubMed: 9334277]

Steventon B, Mayor R, & Streit A (2014). Neural crest and placode interaction during the development of the cranial sensory system. Developmental Biology, 389, 28–38. [PubMed: 24491819]

Straub BK, Rickelt S, Zimbelmann R, Grund C, Kuhn C, Iken M, … Franke WW (2011). E-N-cadherin heterodimers define novel adherens junctions connecting endoderm-derived cells. The Journal of Cell Biology, 195, 873–887. [PubMed: 22105347]

Taneyhill LA, & Schiffmacher AT (2017). Should I stay or should I go?Cadherin function and regulation in the neural crest. Genesis, 55(6), 10.1001/dvg.23028

Theveneau E, Steventon B, Scarpa E, Garcia S, Trepat X, Streit A, & Mayor R (2013). Chase-and-run between adjacent cell populations promotes directional collective migration. Nature Cell Biology, 15, 763–772. [PubMed: 23770678]

Wohrn JC, Nakagawa S, Ast M, Takeichi M, & Redies C (1999).Combinatorial expression of cadherins in the tectum and the sorting of neurites in the tectofugal pathways of the chicken embryo. Neuroscience, 90, 985–1000. [PubMed: 10218798]

Wohrn JC, Puelles L, Nakagawa S, Takeichi M, & Redies C (1998). Cadherin expression in the retina and retinofugal pathways of the chicken embryo. The Journal of Comparative Neurology, 396, 20–38. [PubMed: 9623885]

Wu CY, Hooper RM, Han K, & Taneyhill LA (2014). Migratory neural crest cell alphaN-catenin impacts chick trigeminal ganglia formation. Developmental Biology, 392, 295–307. [PubMed: 24882712]

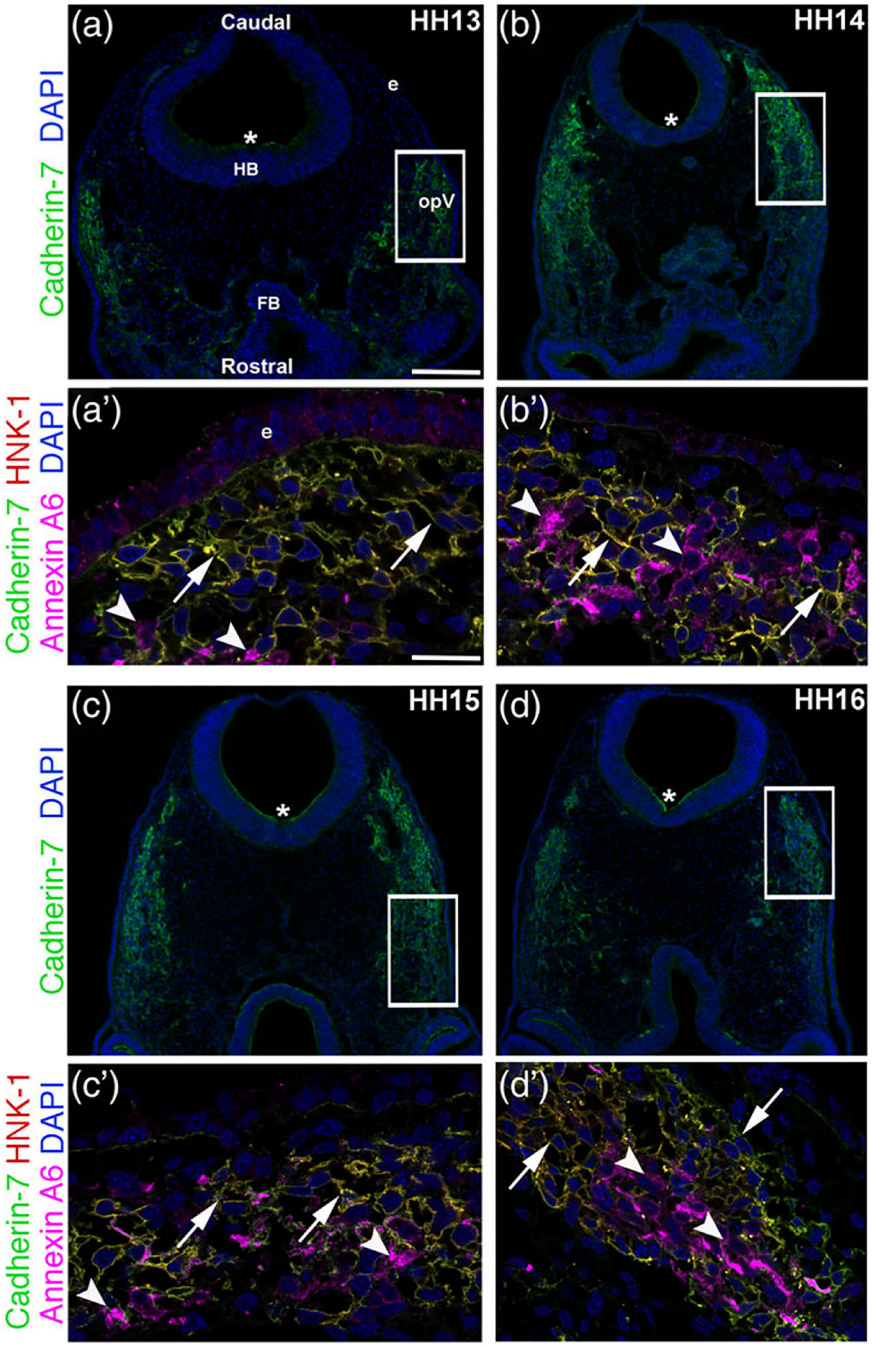

FIGURE 1.

Cadherin-7 protein is observed in migratory neural crest cells contributing to the trigeminal ganglion. Representative transverse sections taken at the axial level of the forming ophthalmic lobe of the trigeminal ganglion over four chick embryo stages (HH13–16) followed by immunohistochemistry for Cadherin-7 (green), HNK-1 (red, labels neural crest cells), and Annexin A6 (purple, labels placodal neurons). (a–d) Lower magnification images show the entire transverse section and reveal Cadherin-7 immunoreactivity, with rostral and caudal orientation, the location of the forebrain (FB), hindbrain (HB), and ectoderm (e), and

the ophthalmic lobe of the trigeminal (opV), indicated in (a) and applicable to (b–d). Asterisk (*) in (a–d) reveals Cadherin-7 immunoreactivity in the neural tube. Higher magnification images (a′–d′) of the boxed area in (a–d) show Cadherin-7-and HNK-1-double-positive neural crest cells at all stages (arrows), whereas Annexin A6-positive placodal neurons are devoid of Cadherin-7 (arrowheads). DAPI (blue) labels cell nuclei. Scale bar in (a) is 100 μm and applicable to (b–d), while scale bar in (a′) is 5 μm and applicable to (b′–d′)

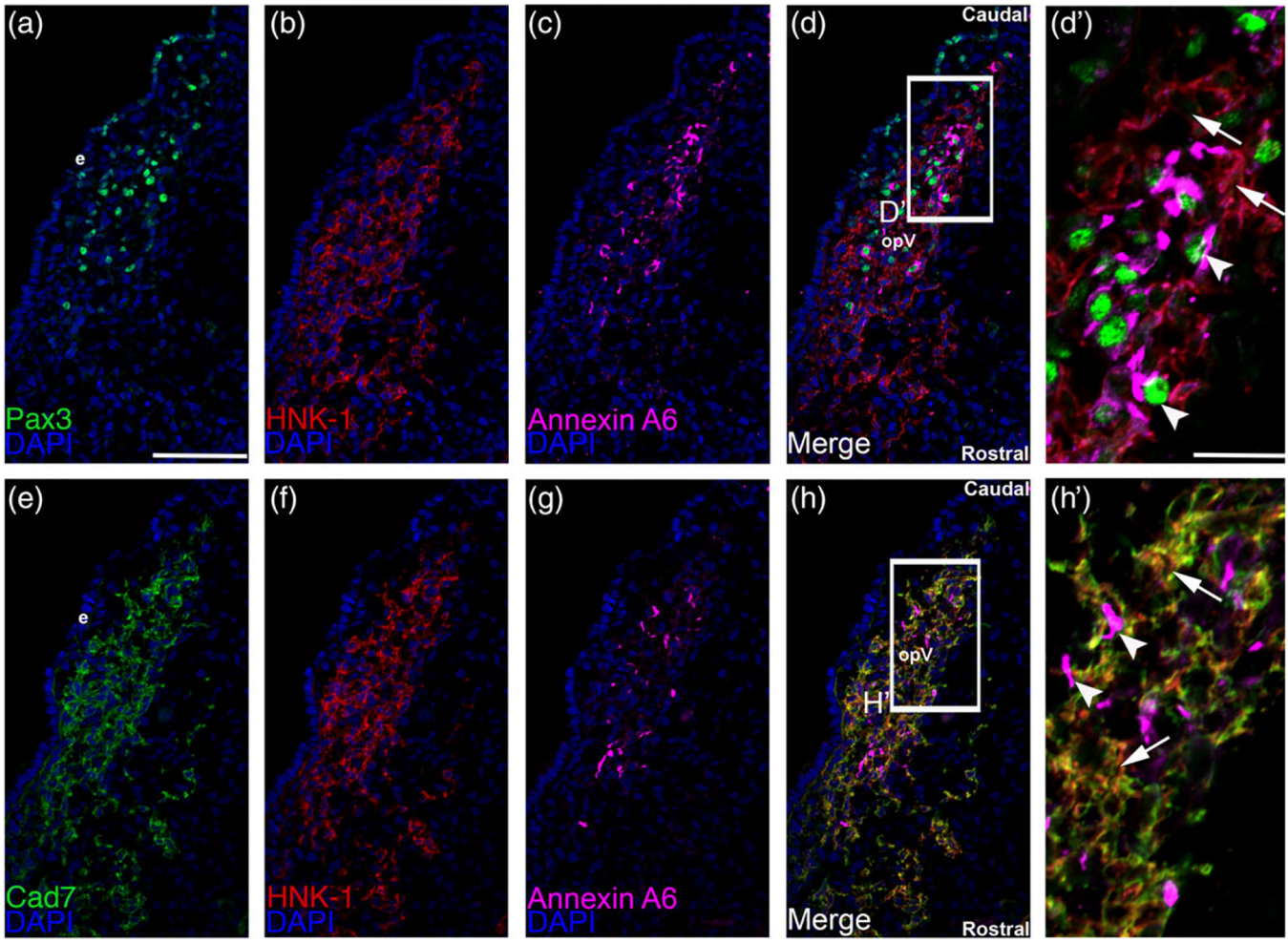

FIGURE 2.

Cadherin-7 protein localizes to HNK1-positive neural crest cells but not Pax3-positive placode cells or placodal neurons. Representative serial/adjacent transverse sections taken at the axial level of the forming ophthalmic lobe of the trigeminal ganglion at HH15 followed by triple-label immunohistochemistry for either Pax3 (a, green), HNK-1 (b, red), and Annexin A6 (c, purple), or Cadherin-7 (e, green), HNK-1 (f, red), and Annexin A6 (g, purple). (d′) Higher magnification image of the boxed region in (d) shows placode cells or placodal neurons (Pax-3- and Annexin A6-positive cells, arrowheads) that are not labeled with HNK-1 and thus are different from HNK-positive neural crest cells (arrows). (h′) Higher magnification image of the boxed region in (h) reveals Cadherin-7 immunoreactivity solely in HNK-1-positive neural crest cells (arrows), while Annexin A6-positive placodal neurons (arrowheads) are devoid of Cadherin-7. Rostral and caudal orientation and the ophthalmic lobe of the trigeminal (opV) are indicated in (d) and (h). DAPI (blue) labels cell nuclei. e = ectoderm. Scale bar in (a) is 67 μm and applicable to (b–h), while scale bar in (d′) is 20 μm and applicable to (h′)

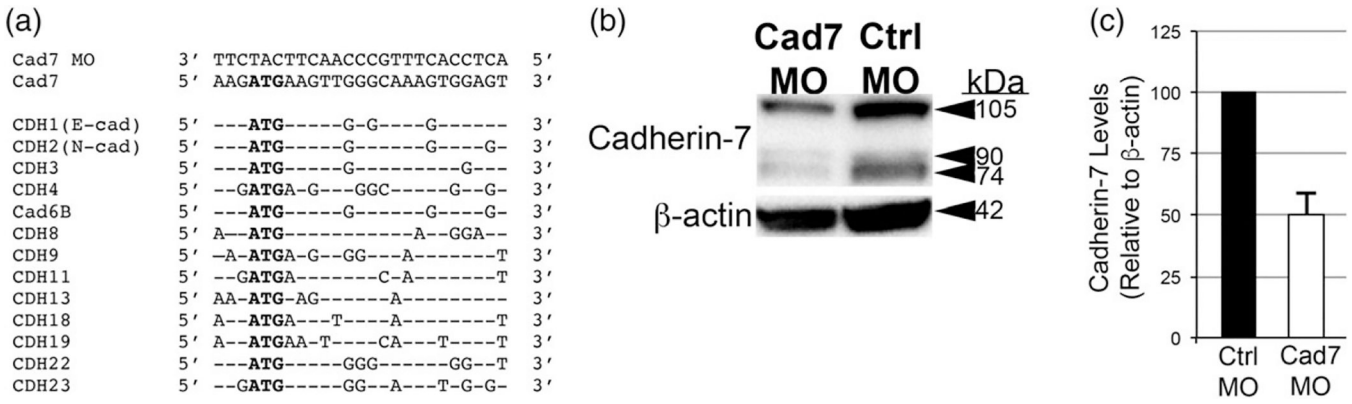

FIGURE 3.

Knockdown of Cadherin-7 with a translation-blocking morpholino antisense oligonucleotide targeting Cadherin-7 effectively reduces Cadherin-7 protein in migratory neural crest cells contributing to the trigeminal ganglion. (a) Comparison of Cadherin-7 MO (Cad7 MO) sequence to the targeting sequence in the Cadherin-7 transcript and to other Cadherin transcripts with expression patterns in premigratory and/or migratory neural crest cells, the neural tube, and in the region of the forming trigeminal ganglion. (b) Premigratory neural crest cells were electroporated at the 2–3ss with either the Cadherin-7 morpholino (Cad7 MO) to allow for depletion of Cadherin-7 protein in migratory neural crest cells, or a 5 bp mismatch Cadherin-7 control MO (Ctrl MO). Embryos were re-incubated to HH15–17 after which time the trigeminal ganglion-forming region on the electroporated side of the embryo was dissected out of the embryo and pooled for lysate preparation. Immunoblotting for Cadherin-7 and β-actin (control) was performed as in (Shah, Schiffmacher, & Taneyhill, 2017), with a representative immunoblot shown. (c) Knockdown efficiency of the Cad7 MO was assessed as previously described (Shah et al., 2017), with graph revealing results of immunoblot analysis as determined by normalizing Cadherin-7 to β-actin and calculating the reduction in this normalized ratio from that obtained for the control MO-treated lysate (arbitrarily set to 1, n = 2). The mean and standard error of the mean are shown. A 50% knockdown in Cadherin-7 protein levels is noted in the Cadherin-7 MO-treated lysate compared to the control MO-treated lysate

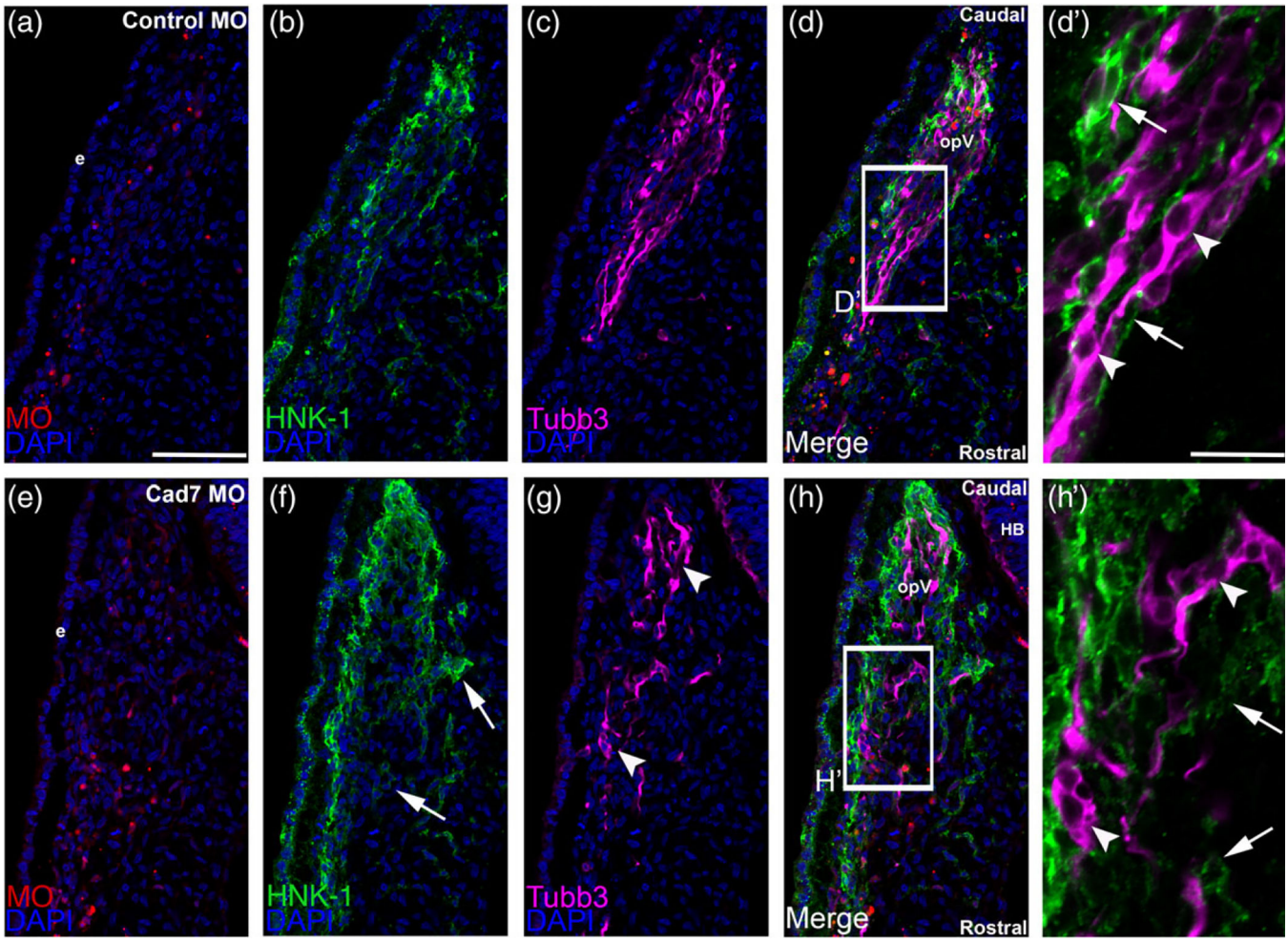

FIGURE 4.

Morpholino-mediated depletion of Cadherin-7 from migratory cranial neural crest cells alters the distribution of neural crest cells and placodal neurons within the forming trigeminal ganglion. Representative transverse sections taken at the axial level of the forming ophthalmic lobe of the trigeminal ganglion after electroporation of a 5 bp mismatch control Cadherin-7 morpholino (control MO, a–d′) or Cadherin-7 MO (Cad7 MO, e–h′) into premigratory neural crest cells at the 3ss followed by immunohistochemistry for HNK-1 (green) and Tubb3 (purple) at HH15. (d′, h′) Higher magnification images of the boxed regions in (d, h). (a–d′) Control MO (a)-containing neural crest cells (b) coalesce with placodal neurons (c, d). At higher magnification (d′), HNK-1-positive neural crest cells (arrows) surround Tubb3-positive placodal neurons (arrowheads), many of which are already forming neurites or adopting the bipolar morphology associated with neuronal maturation. Conversely, a trigeminal ganglion containing the Cadherin-7 MO (e) in the neural crest (f) reveals differences in neural crest cell (f, h, arrows) and placodal neurons (g, h, arrowheads) distribution within the anlage, with neural crest cells sometimes appearing more dispersed compared to control. At higher magnification (h′), it is apparent that neural crest cells still surround the placodal neurons (arrows), but the shape adopted by the placodal neurons is aberrant, with neurons appearing round (arrowheads). Rostral and caudal orientation, the

hindbrain (HB), and the ophthalmic lobe of the trigeminal ganglion (opV) are indicated in (d) and (h). DAPI (blue) labels cell nuclei. e = ectoderm. Scale bar in (a) is 67 μm and applicable to (b–h), while scale bar in (d′) is 20 μm and applicable to (h′)

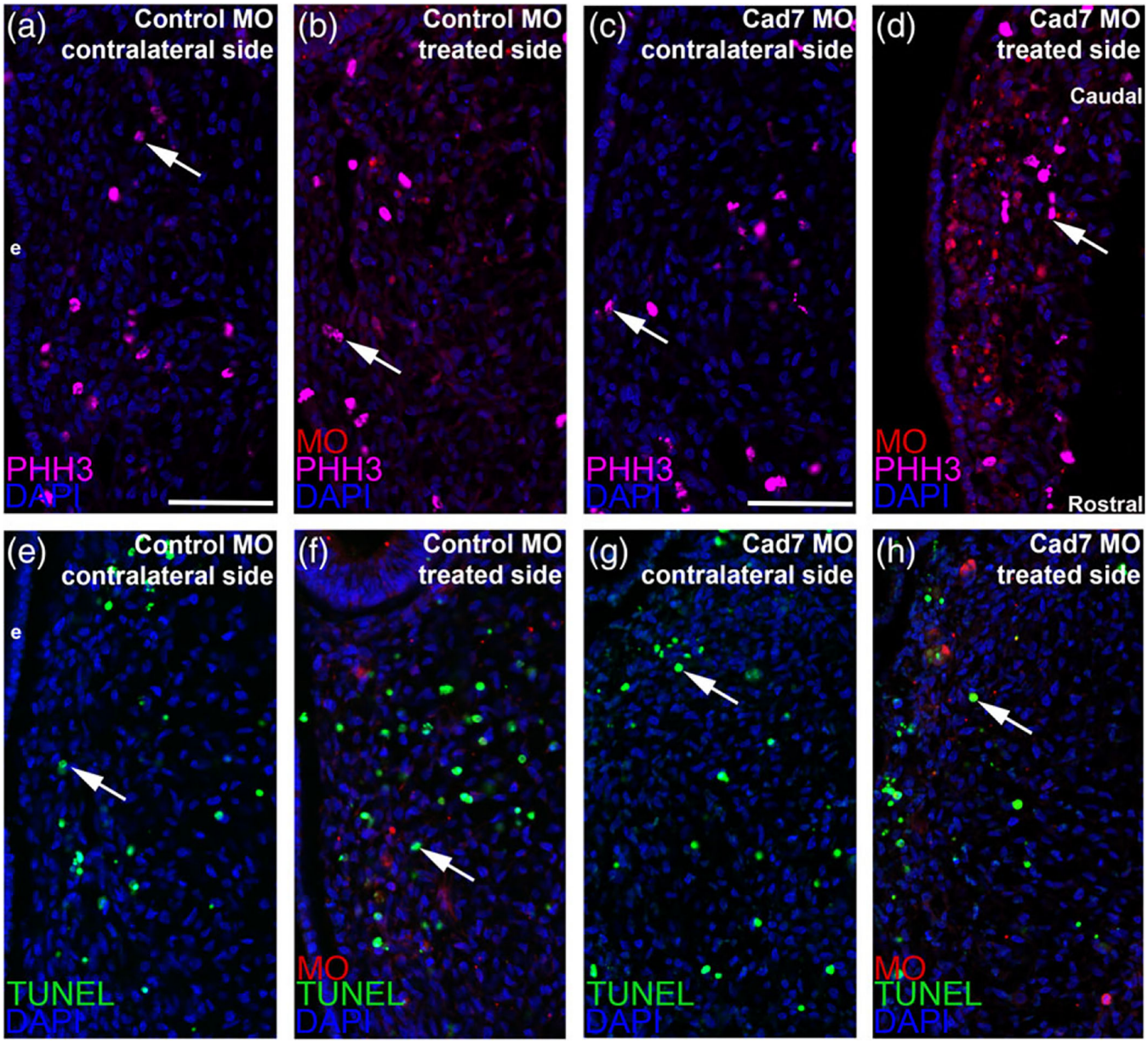

FIGURE 5.

Electroporation of either the control or Cadherin-7 morpholino does not alter cell proliferation or cell death in the trigeminal ganglionic anlage. Representative transverse sections taken at the axial level of the forming ophthalmic lobe of the trigeminal ganglion after electroporation of a 5 bp mismatch control Cadherin-7 morpholino (control MO: a, b, e, f) or Cadherin-7 morpholino (Cad7 MO: c, d, g, h) into premigratory neural crest cells at the 3ss followed by immunohistochemistry for phospho-histone H3 (PHH3, a–d) or TUNEL (e–h) at HH15. Contralateral (a, c, e, g) and morpholino-treated (b, d, f, h) sides are shown to provide a means of comparison. Arrows indicate PHH3 (a–d)- and TUNEL (e–h)-positive nuclei, with a comparable number noted in the presence of either morpholino relative to the contralateral control side of the electroporated embryo. DAPI (blue) labels cell nuclei. Ectoderm (e) is oriented to the left within each image panel and may not be visible in the

field of view for some images. Rostral and caudal orientation is shown in (d) and applies to all images. Scale bar in (a) is 67 μm and applies to (b, e, f), while scale bar in (c) is 50 μm and applies to (d, g, h)

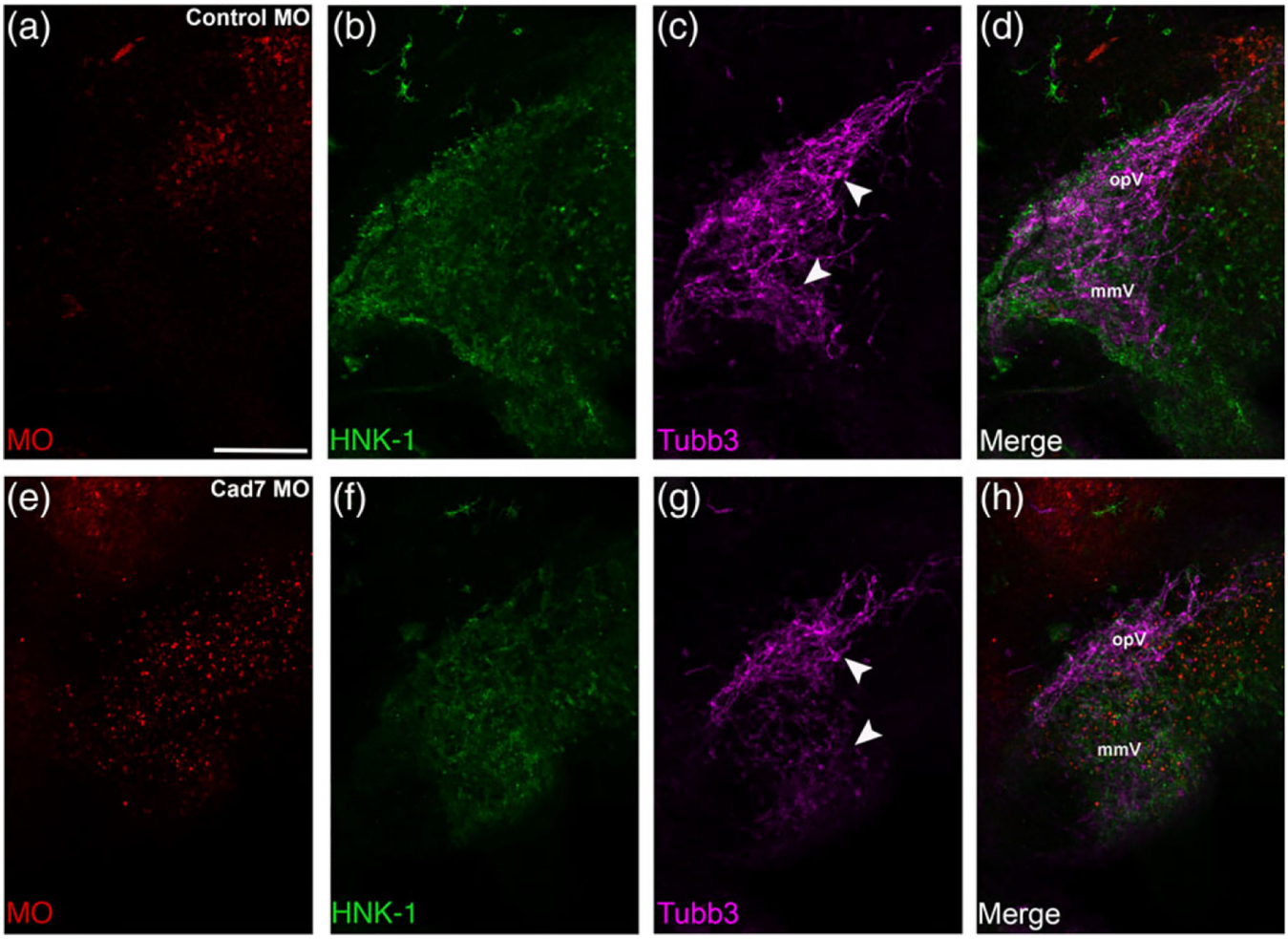

FIGURE 6.

Cadherin-7 depletion in migratory neural crest cells alters the gross morphology of the trigeminal ganglion. Representative lateral views (optical section) of the forming trigeminal ganglion in an HH15 chick head after electroporation of a 5 bp mismatch control Cadherin-7 MO (control MO, a–d) or Cadherin-7 MO (Cad7 MO, e–h) at the 3ss, followed by whole-mount immunohistochemistry for HNK-1 (green) and Tubb3 (purple). Merge images are shown in (d, h). A trigeminal ganglion electroporated with the control MO in neural crest cells (a) exhibits a bilobed morphology, with neural crest cells (b) condensing with placodal neurons (c, arrowheads). A trigeminal ganglion electroporated with the Cadherin-7 MO in the neural crest (e) possesses neural crest cells that migrate to the anlage (f) but placodal neurons do not condense properly (g, arrowheads), leading to an aberrant ganglion shape relative to control. The ophthalmic (opV) and maxillomandibular (mmV) lobes of the trigeminal ganglion are indicated in (d) and (h). Scale bar in (a) is 200 μm and applies to all images

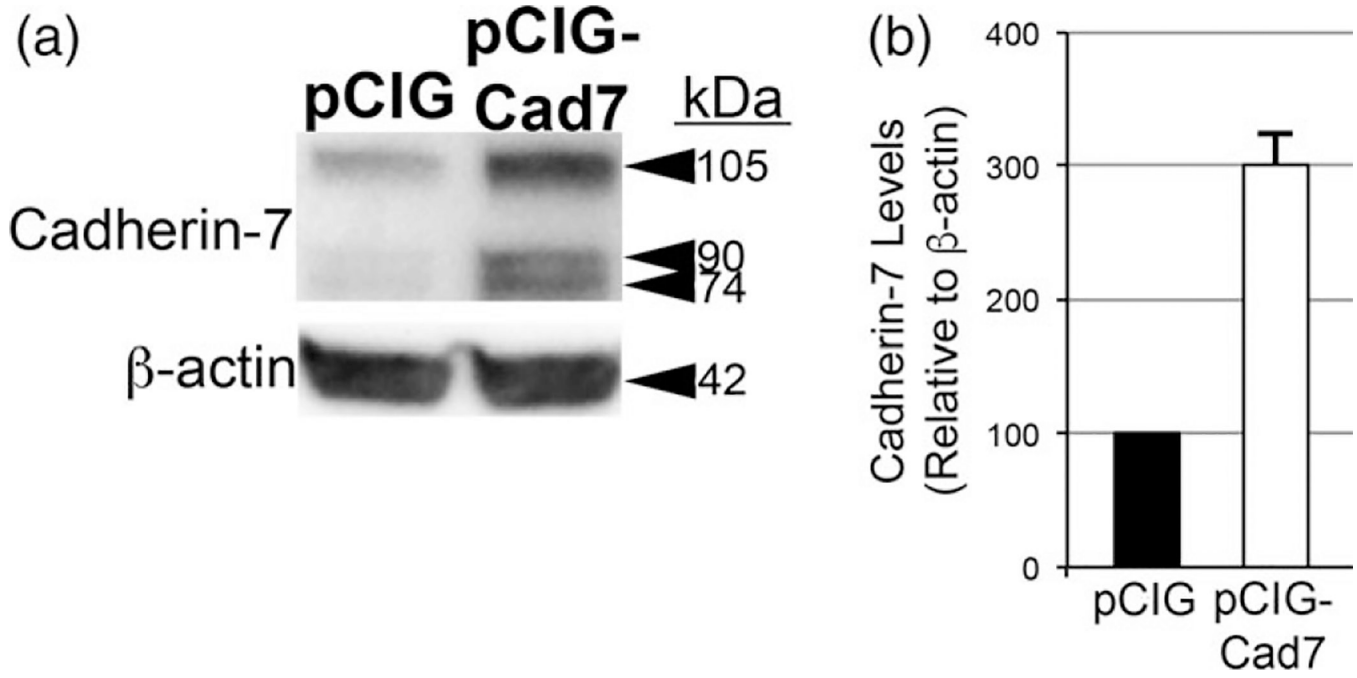

FIGURE 7.

Overexpression of Cadherin-7 effectively increases Cadherin-7 protein in neural crest cells contributing to the trigeminal ganglion. (a) Premigratory neural crest cells were electroporated at 2–3ss with either a Cadherin-7 expression construct (pCIG-Cad7) to allow for overexpression of Cadherin-7 protein in migratory neural crest cells, or the control vector (pCIG). Embryos were re-incubated HH15–17 after which time the trigeminal ganglion-forming region on the electroporated side of the embryo was dissected out of the embryo and pooled for lysate preparation. Immunoblotting for Cadherin-7 and β-actin (control) was performed as in (Shah et al.,2017), with a representative immunoblot shown. (b) Overexpression efficiency was assessed as previously described (Shah et al., 2017), with graph indicating results of immunoblot analysis as determined by normalizing Cadherin-7 to β-actin and calculating the increase in this normalized ratio from that obtained for the pCIG-treated lysate (arbitrarily set to 1, n = 2). The mean and standard error of the mean are shown. A 200% increase in Cadherin-7 protein levels is noted in the pCIG-Cad7-treated lysate compared to the control pCIG-treated lysate

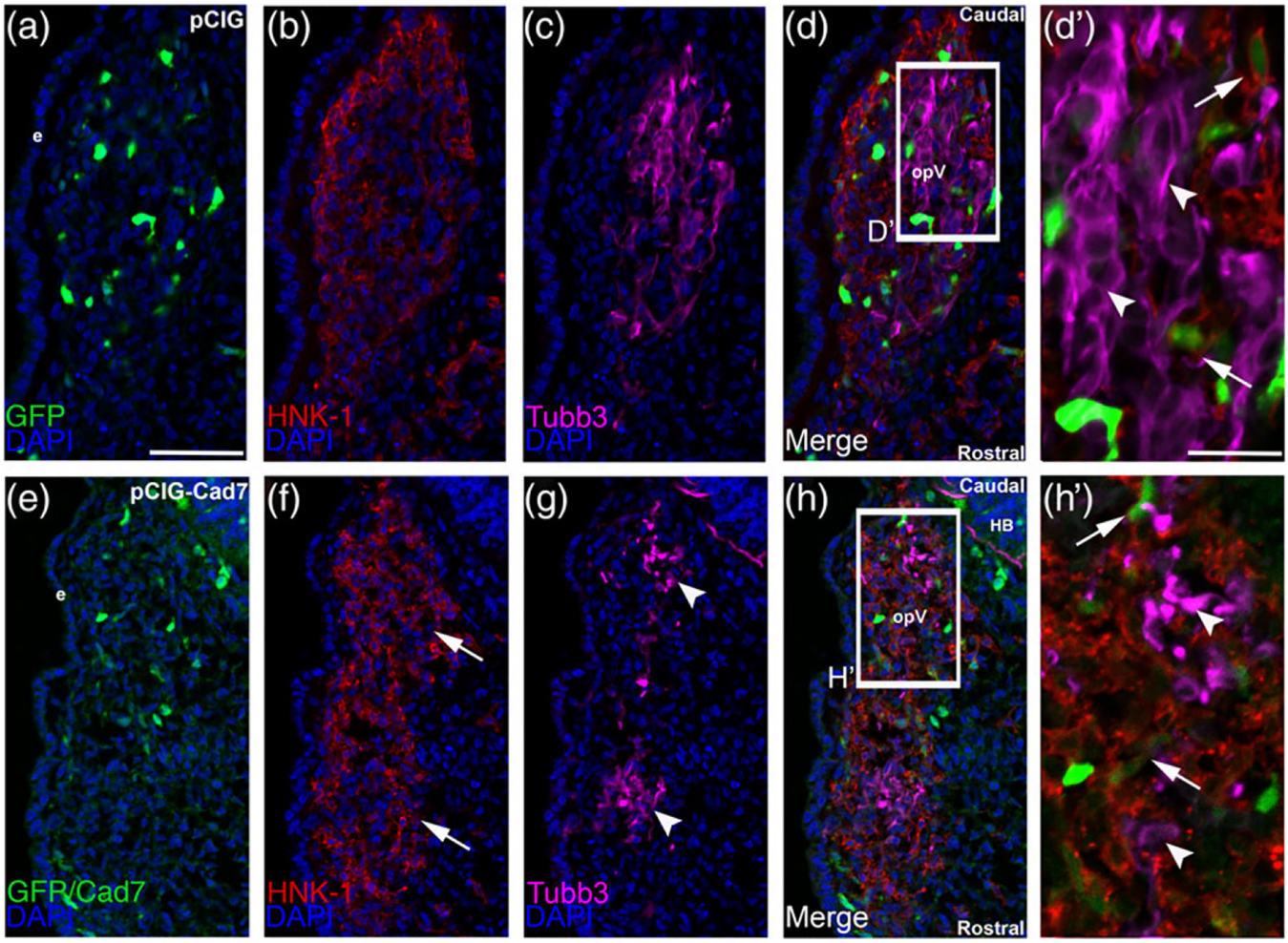

FIGURE 8.

Overexpression of Cadherin-7 in migratory cranial neural crest cells alters the distribution of neural crest cells and placodal neurons within the forming trigeminal ganglion. Representative transverse sections taken at the axial level of the forming ophthalmic lobe of the trigeminal ganglion after electroporation of the pCIG control vector (pCIG, a–d′) or the pCIG-Cadherin-7 vector (pCIG-Cad7, e–h′) into premigratory neural crest cells at the 3ss followed by immunohistochemistry for HNK-1 (red) and Tubb3 (purple) at HH15. The pCIG vector contains an IRES-GFP cassette to label electroporated cells. (d′, h′) Higher magnification images of the boxed regions in (d, h). (a–d′) pCIG control vector (a)-containing neural crest cells (b) coalesce with placodal neurons (c, d). At higher magnification (d′), HNK-1-positive neural crest cells (arrows) form corridors around Tubb3-positive placodal neurons (arrowheads), many of which are elaborating neurites indicative of neuronal maturation. On the other hand, neural crest cells with elevated levels of Cadherin-7 protein (e) migrate to the ganglionic anlage (f, arrows) but likely localize there incorrectly given the inappropriate positioning of placodal neurons (g, arrowheads). At higher magnification (h′), neural crest cells are noted around the placodal neurons (arrows), but placodal neuron morphology is abnormal, with neurons appearing round and/or misshapen (arrowheads). Rostral and caudal orientation, the hindbrain (HB), and the ophthalmic lobe of

the trigeminal (opV) are indicated in (d) and (h). DAPI (blue) labels cell nuclei. e = ectoderm. Scale bar in (a) is 50 μm and applicable to (b–h), while scale bar in (d′) is 20 μm and applicable to (h′)

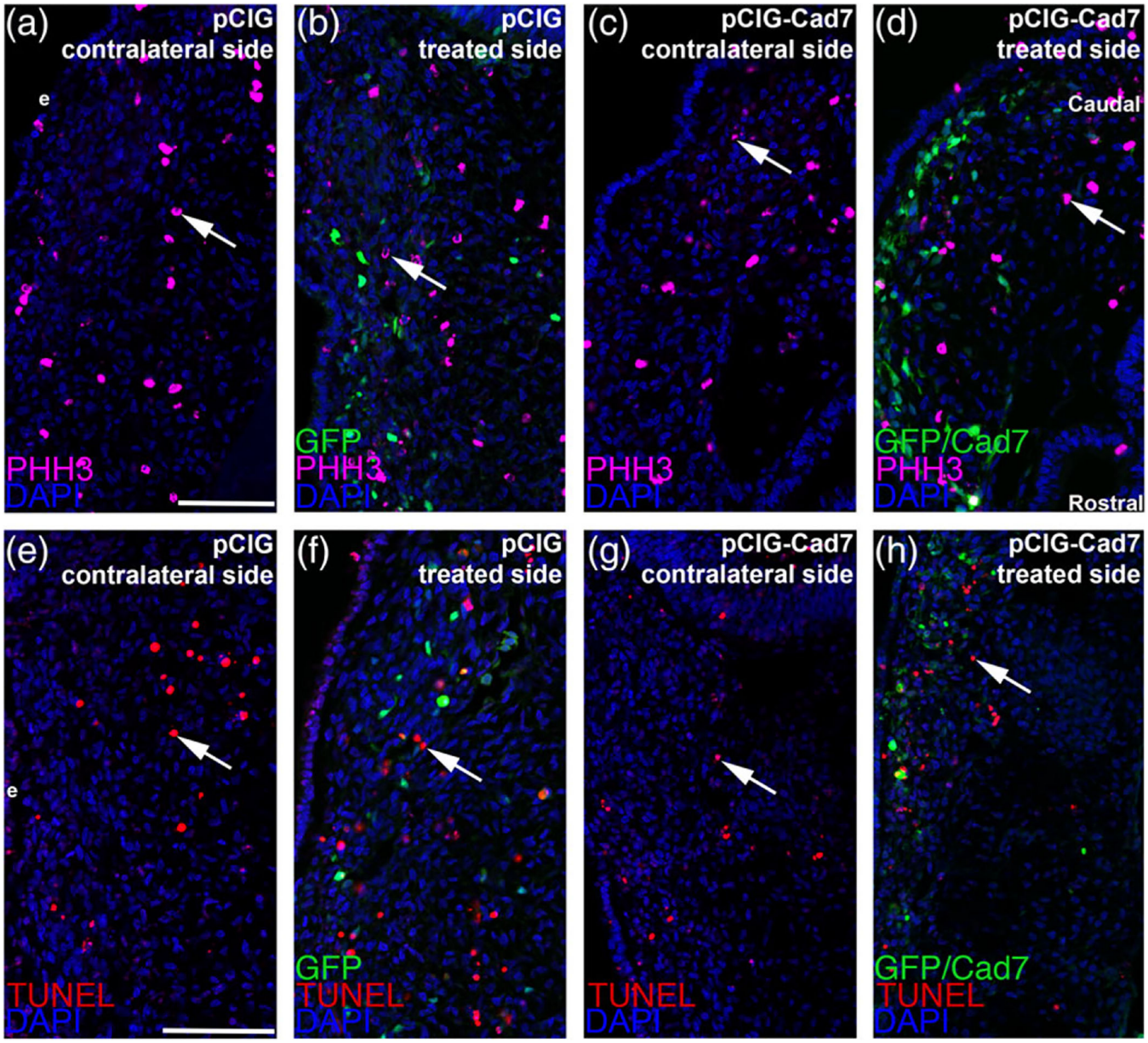

FIGURE 9.

Electroporation of expression constructs does not alter cell death or cell proliferation in the trigeminal ganglionic anlage. Representative transverse sections taken at the axial level of the forming ophthalmic lobe of the trigeminal ganglion after electroporation of the pCIG control vector (pCIG: a, b, e, f) or pCIG-Cadherin-7 vector (pCIG-Cad7: c, d, g, h) into premigratory neural crest cells at the 3ss followed by immunohistochemistry for phospho-histone H3 (PHH3, a–d) or TUNEL (e–h) at HH15. Contralateral (a, c, e, g) and expression vector-treated (b, d, f, h) sides are shown to provide a means of comparison. Arrows indicate PHH3 (a–d)-and TUNEL (e–h)-positive nuclei, with a comparable number noted in the presence of either expression construct relative to the contralateral control side of the electroporated embryo. DAPI (blue) labels cell nuclei. Ectoderm (e) is oriented to the left within each image panel. Rostral and caudal orientation is shown in (d) and applies to all

images. Scale bar in (a) is 60 μm and applies to (b–d), while scale bar in (e) is 60 μm and is applies to (f–h)

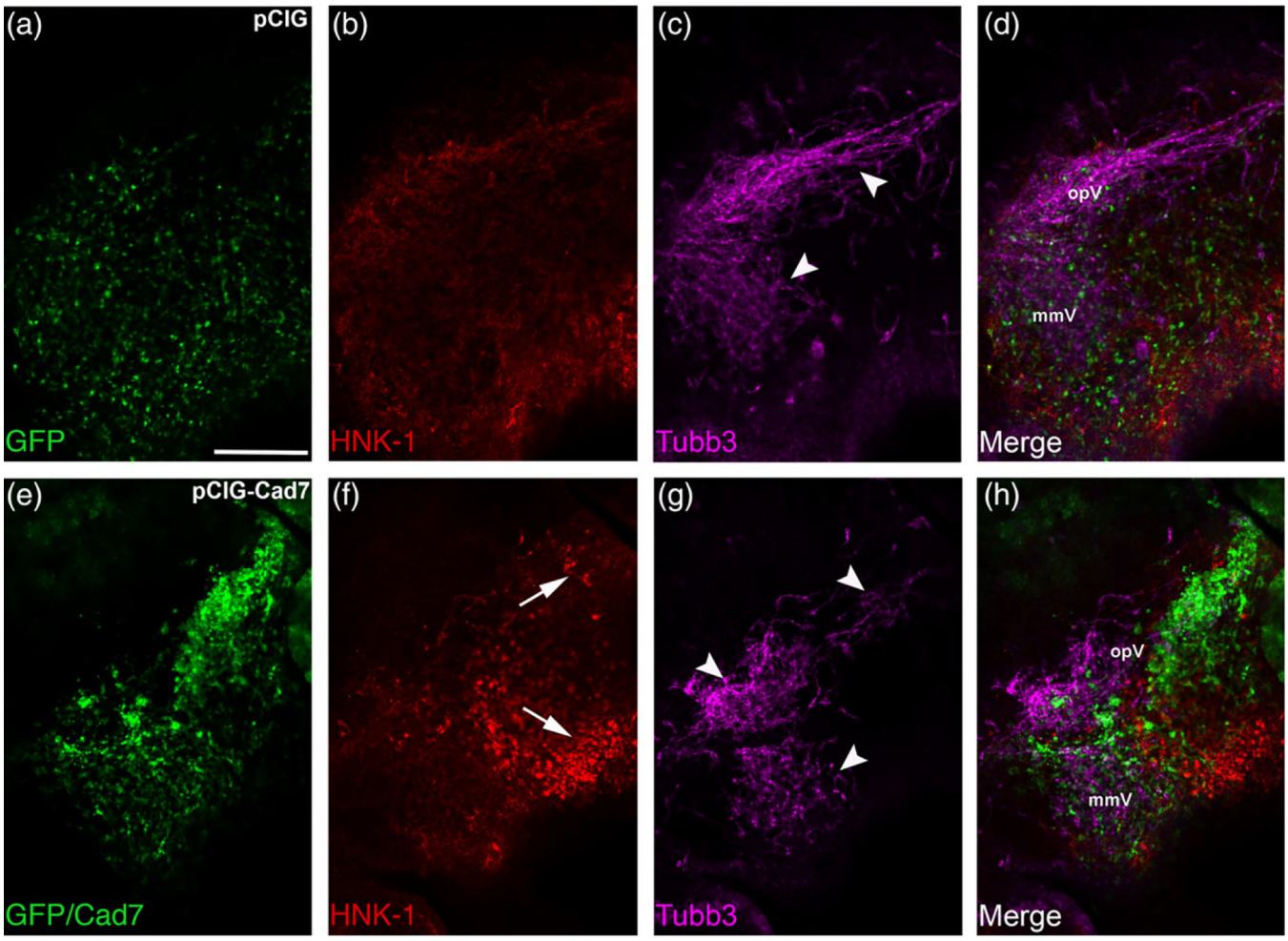

FIGURE 10.

Elevated levels of Cadherin-7 in migratory neural crest cells alter the gross morphology of the trigeminal ganglion. Representative lateral views (optical section) of the forming trigeminal ganglion in an HH15 chick head after electroporation of the pCIG control vector (pCIG, a–d) or the pCIG-Cadherin-7 vector (pCIG-Cad7, e–h) at the 3ss, followed by whole-mount immunohistochemistry for HNK-1 (red) and Tubb3 (purple). Merge images are shown in (d, h). A trigeminal ganglion electroporated with the control pCIG vector in neural crest cells (a) exhibits a bilobed morphology, with neural crest cells (b) coalescing with placodal neurons (c, arrowheads). A trigeminal ganglion electroporated with pCIG-Cad7 in the neural crest (e) possesses neural crest cells that migrate to the anlage, but these cells appear to aggregate together, thus altering their general distribution in the anlage (e, f, arrows). Placodal neurons are also affected, exhibiting a less compact appearance (g, arrowheads). Together, this leads to an abnormal ganglion shape relative to control. The ophthalmic (opV) and maxillomandibular (mmV) lobes of the trigeminal ganglion are indicated in (d) and (h). Scale bar in (a) is 200 μm and applies to all images